

We are IntechOpen, the world's leading publisher of Open Access books Built by scientists, for scientists

6,900

Open access books available

186,000

International authors and editors

200M

Downloads

Our authors are among the

154

Countries delivered to

TOP 1%

most cited scientists

12.2%

Contributors from top 500 universities



WEB OF SCIENCE™

Selection of our books indexed in the Book Citation Index
in Web of Science™ Core Collection (BKCI)

Interested in publishing with us?
Contact book.department@intechopen.com

Numbers displayed above are based on latest data collected.
For more information visit www.intechopen.com



Darcy-Forchheimer Flow of Casson Nanofluid with Heat Source/Sink: A Three-Dimensional Study

Gosikere Kenchappa Ramesh

Additional information is available at the end of the chapter

<http://dx.doi.org/10.5772/intechopen.74170>

Abstract

In this chapter, three-dimensional Casson nanoliquid flow in two lateral directions past a porous space by Darcy-Forchheimer articulation is examined. The study includes the impact of uniform heat source/sink and convective boundary condition. The administering partial differential equations are shaped to utilizing comparability changes into a set of nonlinear normal differential conditions which are fathomed numerically. The self-comparative arrangements are gotten and contrasted and accessible information for uncommon cases. The conduct of parameters is displayed graphically and examined for velocity, temperature, and nanoparticle volume part. It is discovered that temperature and nanoparticle volume fraction rise for enhancement of Forchheimer and porosity parameters.

Keywords: three-dimensional flow, Darcy-Forchheimer porous medium, Casson nanoliquid, uniform heat source/sink, convective boundary condition, numerical solutions

1. Introduction

In many assembling processes and for mechanical reason, the investigation of heat exchange and boundary layer flow over linearly and nonlinearly extending surface are much imperative. These procedures and applications incorporate streamlined feature forming, wire drawing, and paper generation where a specific temperature will be required for cooling the particles in the liquid. At first, the stream qualities have been analyzed by [1] overextending surfaces. The perfection of finishing up item relies upon the rate of warmth exchange at the surface of extending material. Many creators expanded crafted by [1] managed heat exchange qualities alongside the flow conduct in different physical circumstances in [2–8].

Non-Newtonian fluids can't be portrayed because of nonexistence of single constitutive connection among stress and rate of strain. In the current year, non-Newtonian fluids have turned out to be increasingly essential because of its mechanical applications. Truth be told, the enthusiasm for boundary layer flows of non-Newtonian fluid is expanding significantly because of its extensive number of functional applications in industry producing preparing and natural fluids. Maybe, a couple of principle illustrations identified with applications are plastic polymer, boring mud, optical fibers, paper generation, hot moving, metal turning, and cooling of metallic plates in a cooling shower and numerous others. Since no single non-Newtonian model predicts every one of the properties of non-Newtonian fluid along these lines examinations proposed different non-Newtonian fluid models. These models are essentially classified into three classifications specifically differential-, rate-, and fundamental-type fluids. In non-Newtonian fluid, shear stresses and rates of strain/disfigurement are not directly related. Such fluid underthought which does not comply with Newton's law is a straightforward non-Newtonian fluid model of respectful sort. In 1959, Casson displayed this model for the flow of viscoelastic fluids. This model has a more slow progress from Newtonian to the yield locale. This model is utilized by oil builds in the portrayal of bond slurry and is better to predict high shear-rate viscosities when just low and middle road shear-rate information are accessible. The Casson show is more exact at both high and low shear rates. Casson liquid has one of the kind attributes, which have wide application in sustenance handling, in metallurgy, in penetrating operation and bio-designing operations, and so on. The Casson show has been utilized as a part of different businesses to give more exact portrayal of high shear-rate viscosities when just low and moderate shear-rate information are accessible [9]. Toward the starting Nadeem et al. [10] introduce the idea of Casson fluid and demonstrate over an exponentially extending sheet. Numerous examinations identified with viscoelastic properties of liquid are underthought [11–17].

The nanoparticles in by and large are made of metal oxides, metallic, carbon, or some other materials [18]. Standard fluid has weaker conductivity. This weaker conductivity can be enhanced incredibly with the utilization of nanoparticles. Truly, the Brownian movement factor of nanoparticles is base fluid and is essential toward this path. An extraordinary measure of warmth is delivered in warm exchangers and microelectromechanical procedures to lessen the framework execution. Fluid thermal conductivity is enhanced by nanoparticle expansion just to cool such modern procedures. The nanoparticles have shallow significance in natural and building applications like prescription, turbine sharp-edge cooling, plasma- and laser-cutting procedure, and so on. Sizeable examinations on nanofluids have been tended to in the writing. Buongiorno [19] has investigated the mechanisms of nanofluid by means of snapshot of nanoparticles in customary base fluid. Such instruments incorporate nanoparticle measure, Magnus effect, dormancy, molecule agglomeration, Brownian movement, thermophoresis, and volume portion. Here, we introduce some imperative scientists who have been accounted for by considering the highlights of thermophoretic and Brownian movement [20–27].

In displaying the flow in permeable media, Darcy's law is a standout among the most prominent models. Particularly, flow in permeable media is exceptionally valuable in grain stockpiling, development of water in repositories, frameworks of groundwater, fermentation process, raw petroleum generation, and oil assets. In any case, it is by and large

perceived that Darcy's model may over anticipate the convective streams when the inertial drag and vorticity dissemination coproductive are considered. The expansion of established Darcy demonstrates incorporates inertial drag and vorticity dispersion. To think about the inertial drag and vorticity dispersion, Forchheimer [28] joined the root mean square. Forchheimer's term was named by Muskat [29] and inferred that the consideration of Forchheimer's term is substantial for high Reynolds number. Pal and Mondal [30] examined the hydromagnetic Darcy-Forchheimer flow for variable liquid property. Utilizing HAM strategy, Hayat et al. [31] got the systematic answer for Darcy-Forchheimer stream of Maxwell liquid by considering the Cattaneo-Christov hypothesis. Vishnu Ganesh et al. [32] analyzed the thick and Ohmic dispersals, and the second-order slip consequences for Darcy-Forchheimer flow of nanoliquid past an extending/contracting surface. Scientific model for Darcy-Forchheimer stream of Maxwell fluid with attractive field and convective boundary condition is given by Sadiq and Hayat [33]. Utilizing Keller's box strategy, Ishak et al. [34] numerically examined the magnetohydrodynamic flow and heat exchange exhibitions over an extending cylinder. Mixed convective flow and the related warmth and mass exchange qualities over a vertical sheet immersed in a permeable medium have been explored by Pal and Mondal [35] by considering different impacts, for example, Soret, Dufour, and thermal radiation.

The principle objective here is to uncover the Darcy-Forchheimer connection on a three-dimensional Casson nanofluid flow past a stretching sheet. Heat transfer is handled with regular heat generation/absorption and convective-type boundary condition.

2. Mathematical formulation

Three-dimensional flow of Casson nanofluid filling permeable space by Darcy-Forchheimer connection is considered. Flow is bidirectional extending surface. Nanofluid model depicts the properties of Brownian dispersion and thermophoresis. Concurrent states of heat convective and heat source/sink are executed. We receive the Cartesian coordinate in such a way to the point that and pivot are picked along x and y ordinary to the stretchable surface. Let $U_w(x) = ax$ and $V_w(y) = by$ be the extending velocity along x and y directions separately. The surface temperature is directed by a convective heating procedure which is depicted by heat exchange coefficient h_f and temperature of hot liquid T_f under the surface (see **Figure 1**). The boundary layer equations for flow underthought are

$$\frac{\partial u}{\partial x} + \frac{\partial v}{\partial y} + \frac{\partial w}{\partial z} = 0, \quad (1)$$

$$u \frac{\partial u}{\partial x} + v \frac{\partial u}{\partial y} + w \frac{\partial u}{\partial z} = \nu \left(1 + \frac{1}{\beta}\right) \frac{\partial^2 u}{\partial z^2} - \frac{\nu}{K} u - Fu^2, \quad (2)$$

$$u \frac{\partial v}{\partial x} + v \frac{\partial v}{\partial y} + w \frac{\partial v}{\partial z} = \nu \left(1 + \frac{1}{\beta}\right) \frac{\partial^2 v}{\partial z^2} - \frac{\nu}{K} v - Fv^2, \quad (3)$$

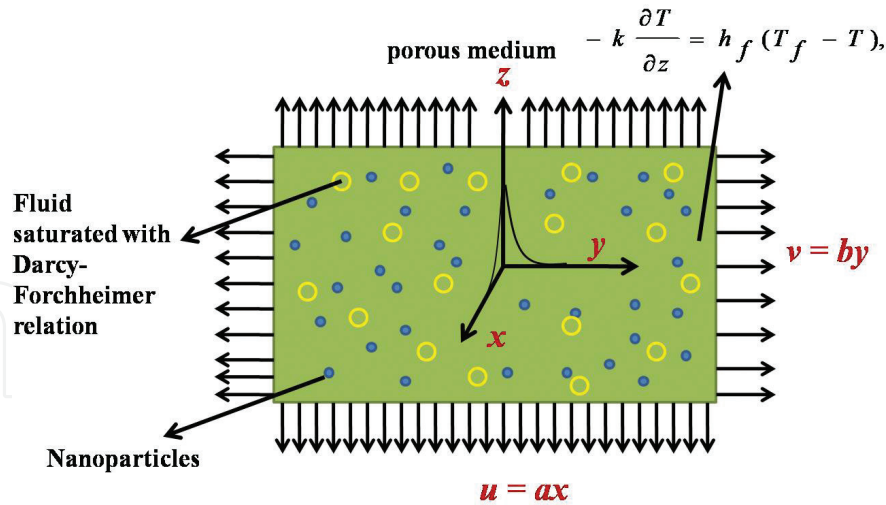


Figure 1. Geometry of the problem.

$$u \frac{\partial T}{\partial x} + v \frac{\partial T}{\partial y} + w \frac{\partial T}{\partial z} = \alpha_m \frac{\partial^2 T}{\partial z^2} + \frac{(\rho c)_p}{(\rho c)_f} \left(D_B \left(\frac{\partial T}{\partial z} \frac{\partial C}{\partial z} \right) + \frac{D_T}{T_\infty} \left(\frac{\partial T}{\partial z} \right)^2 \right) + \frac{q_0}{(\rho c)_p} (T - T_\infty) \quad (4)$$

$$u \frac{\partial C}{\partial x} + v \frac{\partial C}{\partial y} + w \frac{\partial C}{\partial z} = D_B \left(\frac{\partial^2 C}{\partial z^2} \right) + \frac{D_T}{T_\infty} \left(\frac{\partial^2 T}{\partial z^2} \right) \quad (5)$$

and boundary conditions of the problem is

$$u = ax, v = by, w = 0, -k \frac{\partial T}{\partial z} = h_f (T_f - T), C = C_w \text{ at } z = 0$$

$$u \rightarrow 0, v \rightarrow 0, T \rightarrow T_\infty, C \rightarrow C_\infty \text{ as } z \rightarrow \infty \quad (6)$$

Here u, v and w represent as components of velocity in x, y and z directions, respectively; $\nu = \frac{\mu}{\rho_f}$ stands for kinematic viscosity; μ for dynamic viscosity; ρ_f for density of base liquid; K for permeability of porous medium; $F = \frac{C_b}{xk^{\frac{1}{2}}}$ for nonuniform inertia coefficient of porous medium; C_b for drag coefficient; T for temperature; $\alpha_m = \frac{K}{(\rho c)_f}$ for thermal diffusivity; q_0 volumetric rate of heat generation and absorption; β is the Casson parameter; k for thermal conductivity; $(\rho c)_p$ for effective heat capacity of nanoparticles; $(\rho c)_f$ for heat capacity of fluid; C for concentration; D_B for Brownian diffusion coefficient; D_T for thermophoretic diffusion coefficient; T_∞ for ambient fluid temperature; C_∞ for ambient fluid concentration; and a and b for positive constants.

Selecting similarity transformations are

$$u = axf'(\zeta), v = ayg'(\zeta), w = -(av)^{\frac{1}{2}}(f+g),$$

$$\theta(\zeta) = \frac{T - T_\infty}{T_f - T_\infty}, \phi(\zeta) = \frac{C - C_\infty}{C_w - C_\infty}, \zeta = \left(\frac{a}{v}\right)^{\frac{1}{2}} z \quad (7)$$

Applying Eq. (7) in (1) is verified. and Eqs. (2)–(5) are

$$\left(1 + \frac{1}{\beta}\right) f'' + (f + g) f' - f'^2 - \lambda f' - F_r f'^2 = 0 \quad (8)$$

$$\left(1 + \frac{1}{\beta}\right) g'' + (f + g) g' - g'^2 - \lambda g' - F_r g'^2 = 0 \quad (9)$$

$$\theta'' + \text{Pr}((f + g) \theta' + Nb \theta' \phi' + Nt \theta'^2) + \text{Pr} Q \theta(\eta) = 0 \quad (10)$$

$$\phi'' + Le \text{Pr} (f + g) \phi' + \frac{Nt}{Nb} \theta'' = 0 \quad (11)$$

Boundary conditions of Eq. (6) become

$$f(0) = g(0) = 0, f'(0) = 1, g'(0) = \alpha, \theta'(0) = -Bi(1 - \theta(0)), \phi(0) = 1,$$

$$f'(\infty) \rightarrow 0, g'(\infty) \rightarrow 0, \theta(\infty) \rightarrow 0, \phi(\infty) \rightarrow 0 \quad (12)$$

In the above expressions, λ stands for porosity parameter, F_r for Forchheimer parameter, α for ratio parameter, Pr for Prandtl number, Le for Schmidt number, Bi for Biot number, Nt for thermophoresis parameter, Nb for Brownian motion parameter, and Q heat source/sink parameter.

These dimensionless variables are given by

$$\lambda = \frac{\nu}{Ka'} F_r = \frac{C_b}{K^{\frac{1}{2}}}, \alpha = \frac{b}{a'}, \text{Pr} = \frac{\nu}{\alpha_m'}, Le = \frac{\nu}{D_B'}, Q = \frac{q_0}{a \rho c_p'}, Bi = \frac{h_f \sqrt{a'}}{k},$$

$$Nt = \frac{(\rho c)_p D_T (T_f - T_\infty)}{(\rho c)_f \nu T_\infty}, Nb = \frac{(\rho c)_p D_B C_\infty}{(\rho c)_f \nu}.$$

Dimensionless relations of skin friction coefficient, local Nusselt number, and local Sherwood number are as follows:

$$\text{Re}_x^{\frac{1}{2}} C_{fx} = \left(1 + \frac{1}{\beta}\right) f'(0), \left(\frac{x}{y}\right) \text{Re}_y^{\frac{1}{2}} C_{fy} = \alpha \left(1 + \frac{1}{\beta}\right) g''(0),$$

$$\text{Re}_x^{\frac{1}{2}} N u_x = -\theta'(0), \text{ and } \text{Re}_x^{\frac{1}{2}} S u_x = -\phi'(0),$$

where $\text{Re}_x = U_w \frac{x}{\nu}$ and $\text{Re}_y = V_w \frac{y}{\nu}$ depict the local Reynolds numbers.

3. Results and discussion

The correct arrangements do not appear to be achievable for an entire arrangement of Eqs. (8)–(11) with proper limit conditions given in Eq. (12) in light of the nonlinear shape. This reality compels one to get the arrangement of the issue numerically. Suitable likeness change is received to change the overseeing incomplete differential conditions into an arrangement of non-straight customary differential conditions. The resultant limit esteem issue is understood numerically utilizing an efficient fourth-order Runge-Kutta method alongside shooting method (see Ramesh and Gireesha [27]). Facilitate the union examination is available in **Table 1**. For the verification of precision of the connected numerical plan, an examination of the present outcomes compared to the $-\left(1 + \frac{1}{\beta}\right)f''(0)$ and $-\left(1 + \frac{1}{\beta}\right)g''(0)$ (nonappearance of Forchheimer parameter, porosity parameter) with the accessible distributed consequences of Ahmad and Nazar [16] and Nadeem et al. [15] is made and exhibited in **Table 2**, demonstrates a great understanding in this manner give confidence that the numerical outcomes got are precise.

This section is fundamentally arranged to depict the effect of different correlated physical parameters on velocity profiles $f'(\zeta)$, $g'(\zeta)$, temperature profile $\theta(\zeta)$, nanoparticle part $\phi(\zeta)$, skin

ζ	$f(\zeta)$	$f'(\zeta)$	$-f''(\zeta)$
0	0.000000	1.000000	0.763674
1	0.695167	0.456344	0.365768
2	1.008110	0.202536	0.166242
3	1.146071	0.088680	0.073585
4	1.206291	0.038589	0.032175
5	1.232460	0.016746	0.013992
6	1.243809	0.007258	0.006070
7	1.248727	0.003144	0.002630
8	1.250857	0.001362	0.001139
9	1.251780	0.000590	0.000493
10	1.252179	0.000255	0.000213
11	1.252352	0.000111	0.000092
12	1.252427	0.000047	0.000040
13	1.252460	0.000020	0.000017
14	1.252474	0.000008	0.000007
15	1.252480	0.000006	0.000003
16	1.252482	0.000001	0.000001
17	1.252483	0.000000	0.000000

Table 1. Convergence analysis of the present work.

β	$c = 0$	$c = 0.5$	$c = 1.0$
	$-\left(1 + \frac{1}{\beta}\right) f'(0)$	$-\left(1 + \frac{1}{\beta}\right) f''(0)$	$-\left(1 + \frac{1}{\beta}\right) g''(0)$
1	1.414213 [15, 16]	1.545869 [15, 16]	0.657899 [15, 16]
5	1.095445 [15, 16]	1.197425 [15, 16]	0.509606 [15, 16]
1000	1.000499 [15, 16]	1.093641 [15, 16]	0.465437 [15, 16]

Table 2. Current numerical values and validation for friction factor $-\left(1 + \frac{1}{\beta}\right) f'(0)$.

friction coefficient, and the local Nusselt and local Sherwood number through **Figures 2–16**. Give the first focus on the impact of extending parameter (α) on velocity profile as shown in **Figure 2**. It is noticed that for expanding benefits of extending parameter α , it decreases the speed $f'(\zeta)$, while $g'(\zeta)$ fluctuates for different benefits of extending parameter α . It see that for $\alpha = 0$, exhibit wonders lessen the instance of two dimensional linear stretching, while for

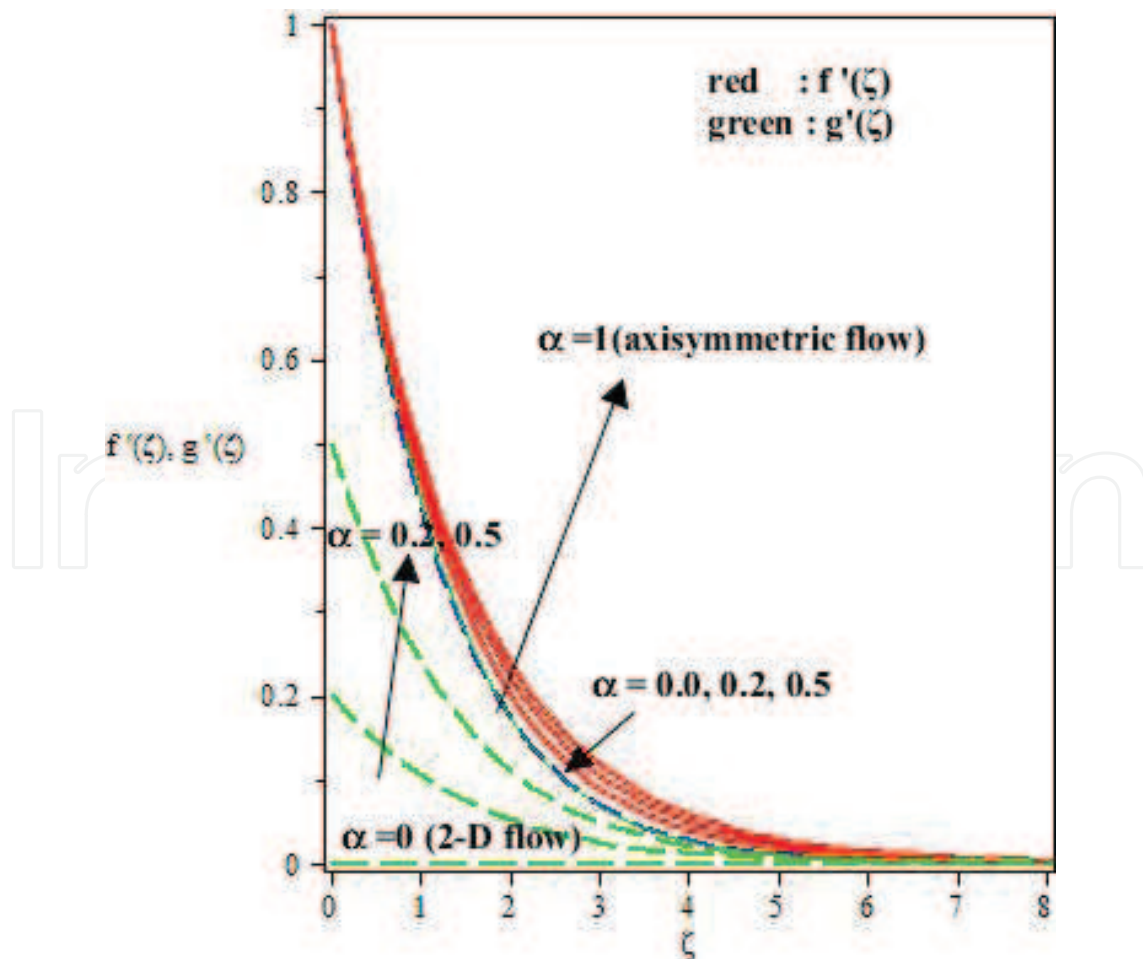


Figure 2. Influence of α on velocity field.

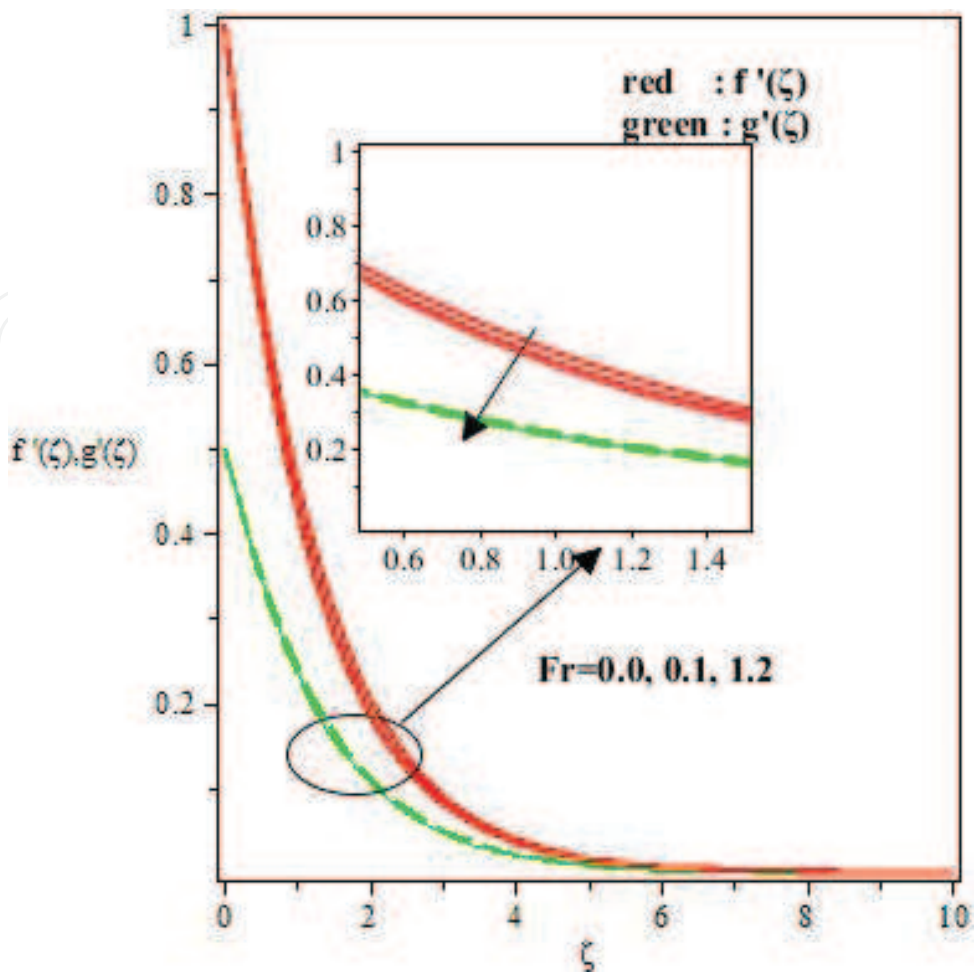


Figure 3. Influence of Fr on velocity fields.

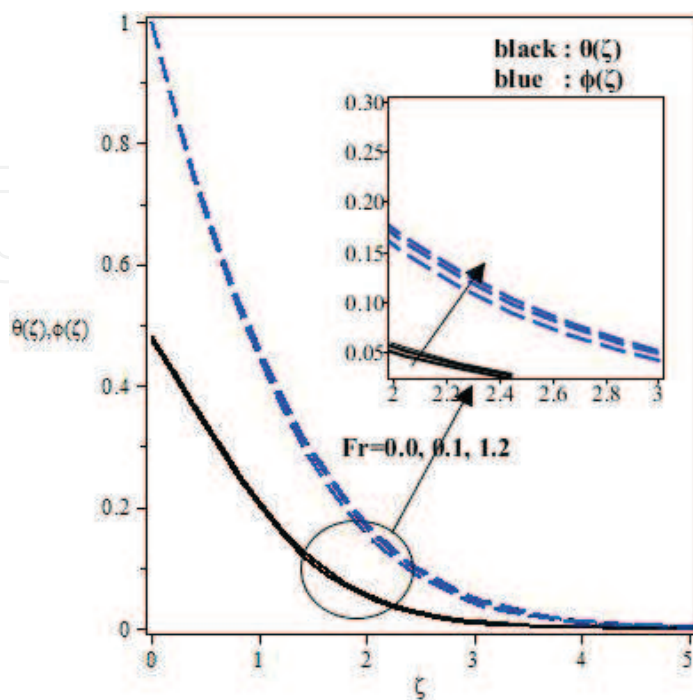


Figure 4. Influence of Fr on temperature and concentration fields.

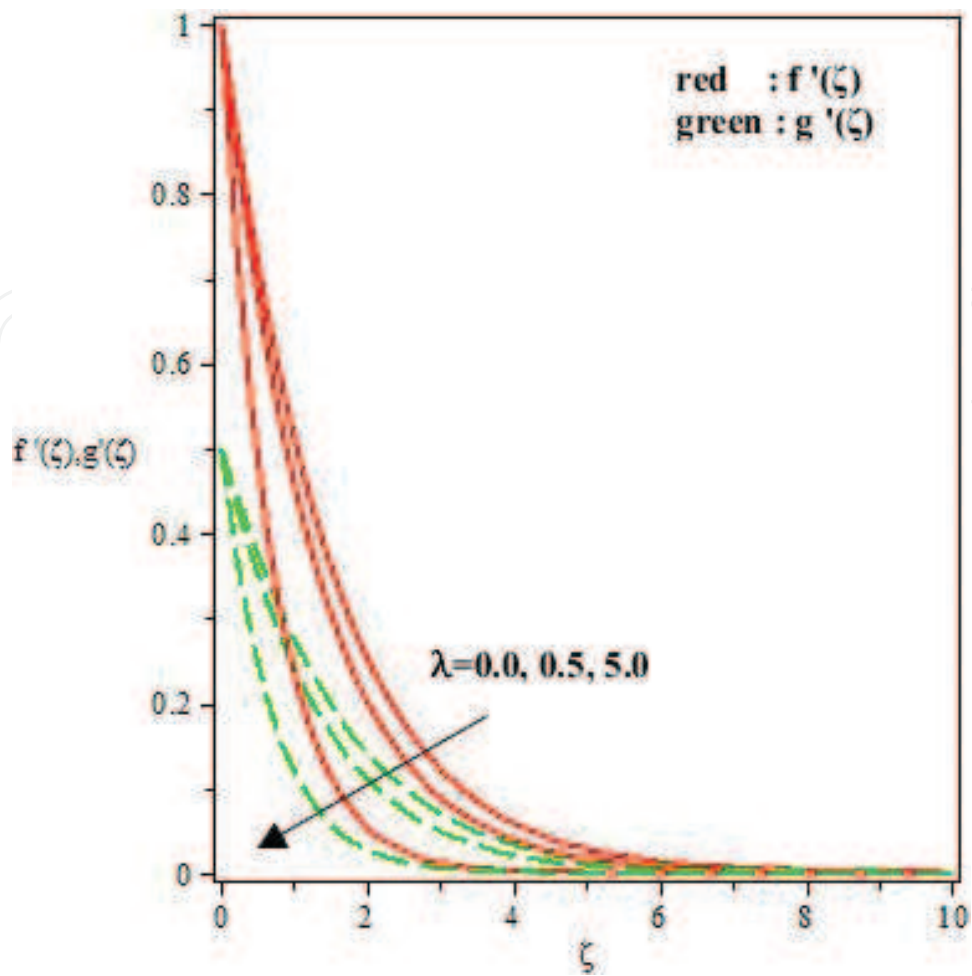


Figure 5. Influence of λ on velocity field.

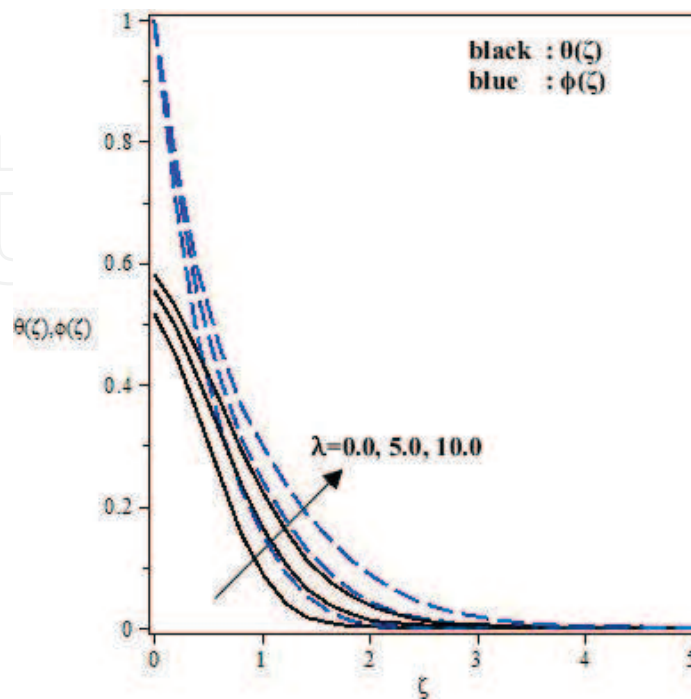


Figure 6. Influence of λ on temperature and concentration fields.

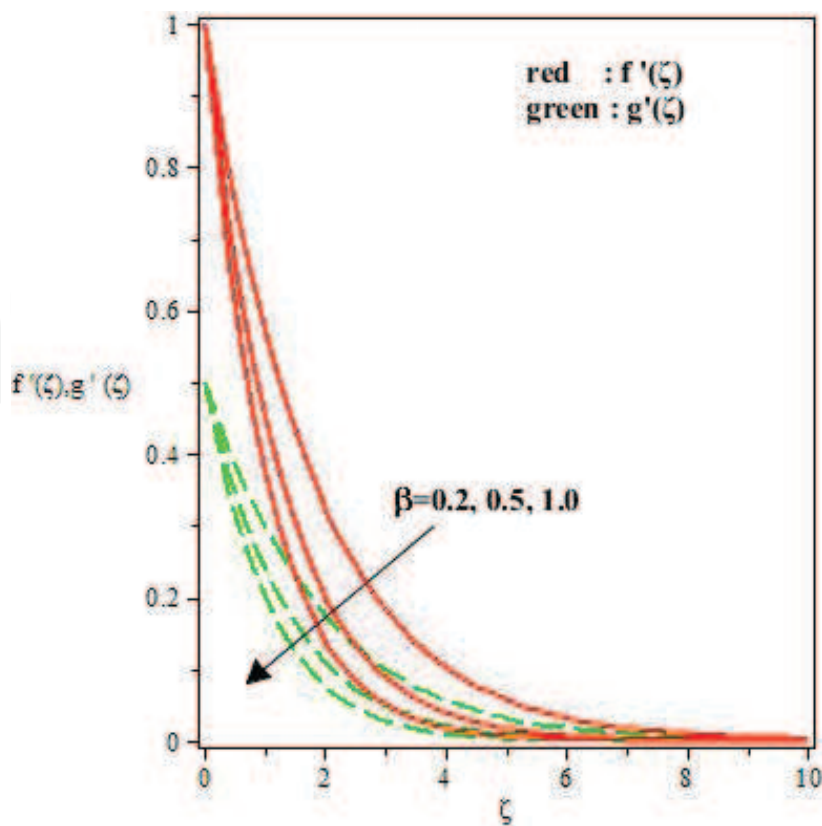


Figure 7. Influence of β on velocity fields.

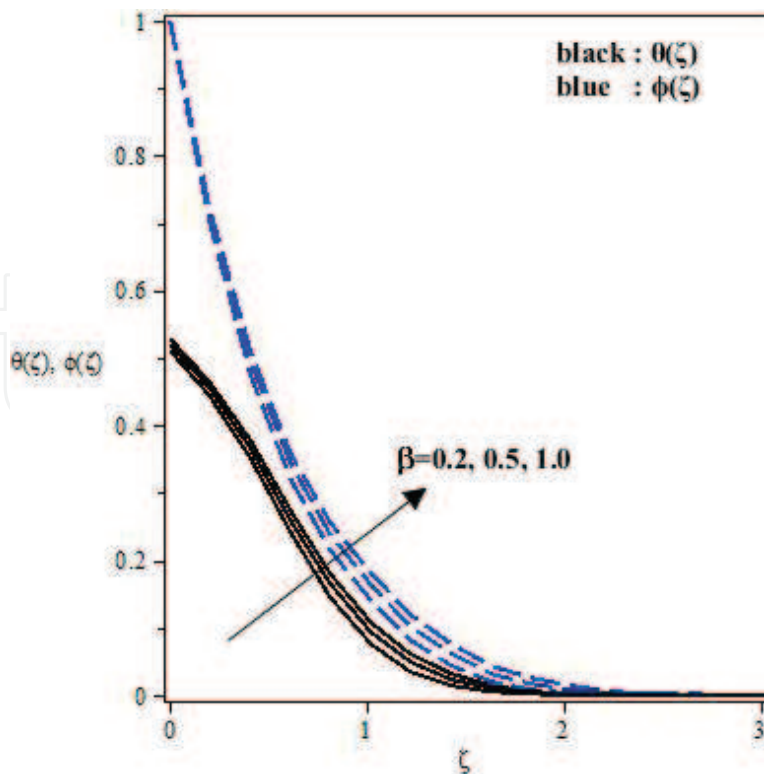


Figure 8. Influence of β on temperature and concentration fields.

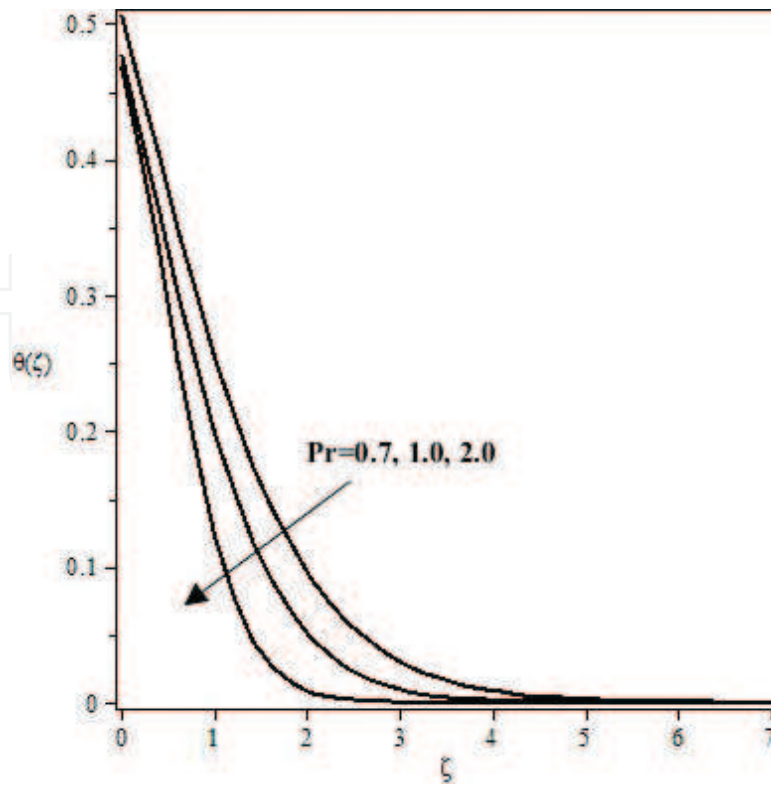


Figure 9. Influence of Pr on temperature fields.

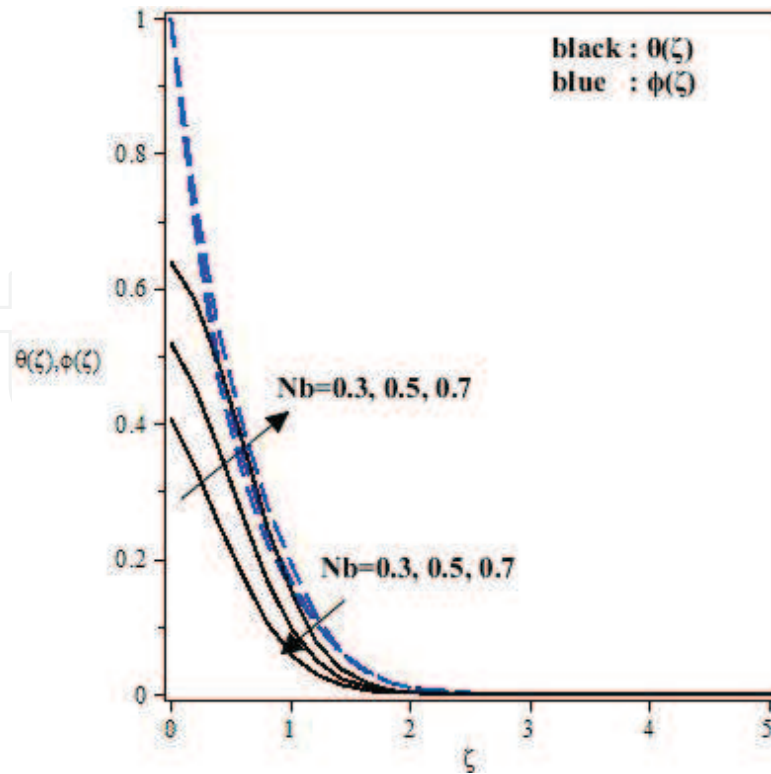


Figure 10. Influence of Nb on temperature and concentration fields.

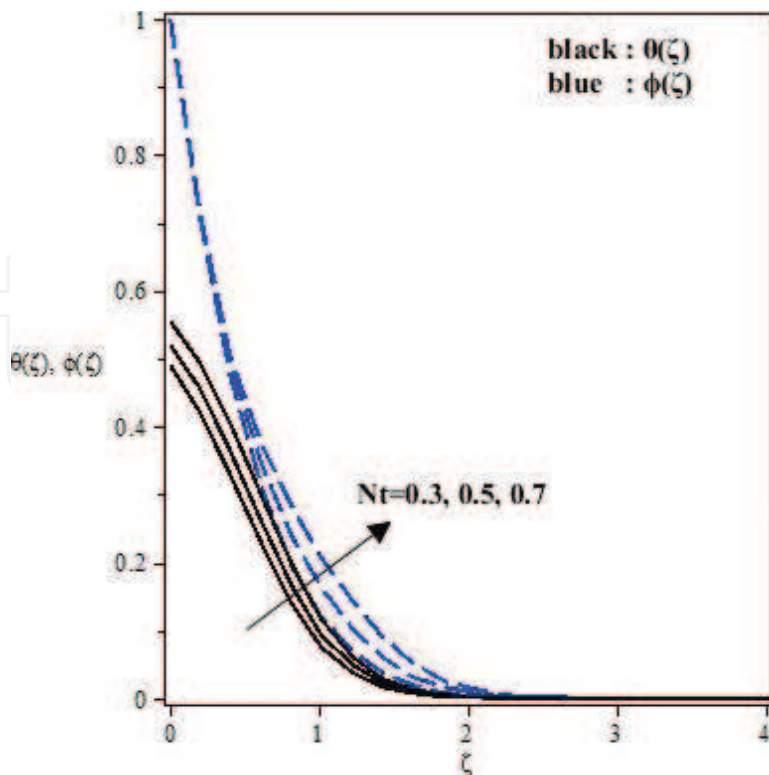


Figure 11. Influence of Nt on temperature and concentration fields.

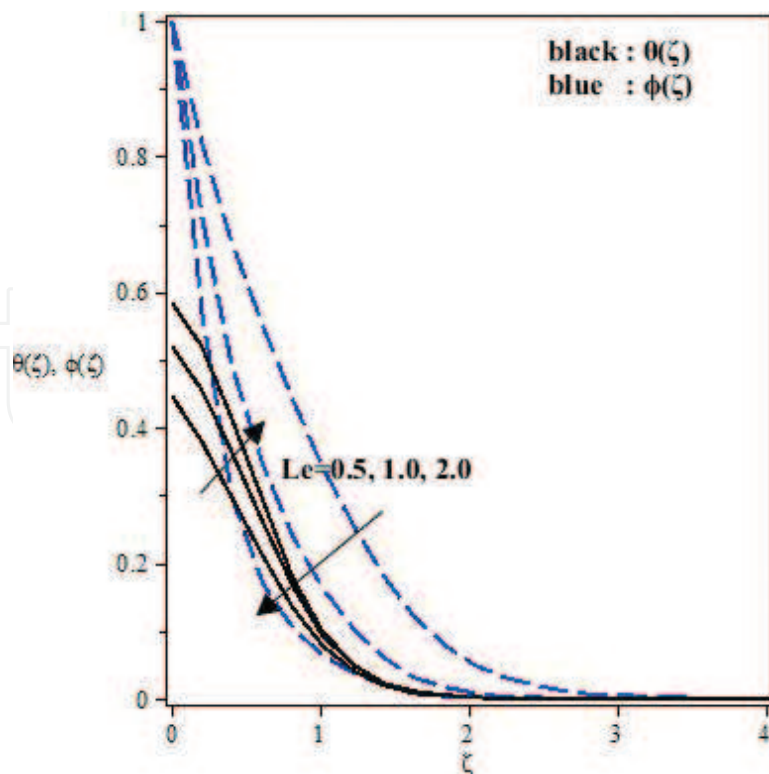


Figure 12. Influence of Le on temperature and concentration fields.

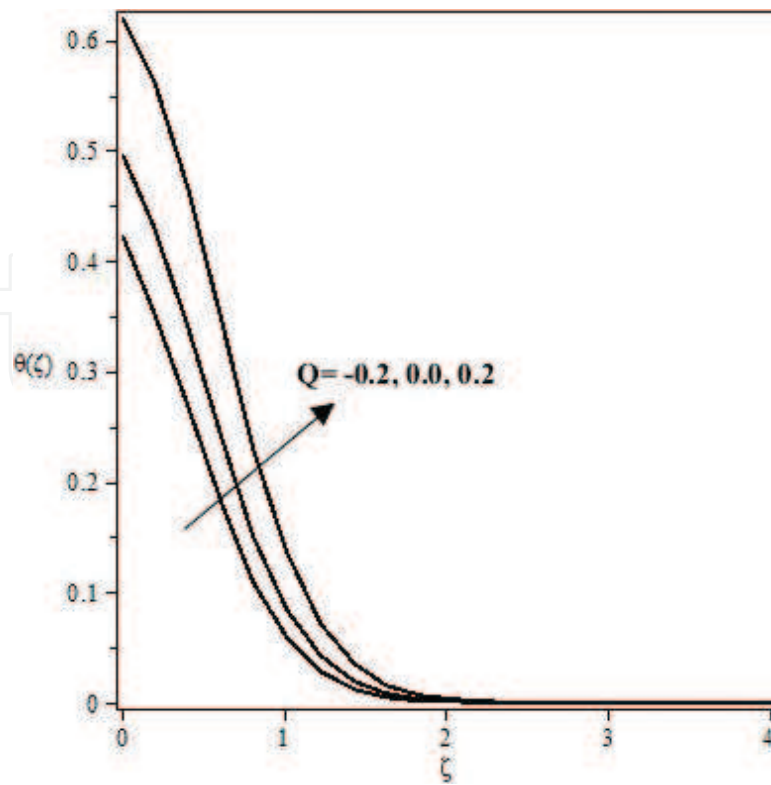


Figure 13. Influence of Q on temperature field.

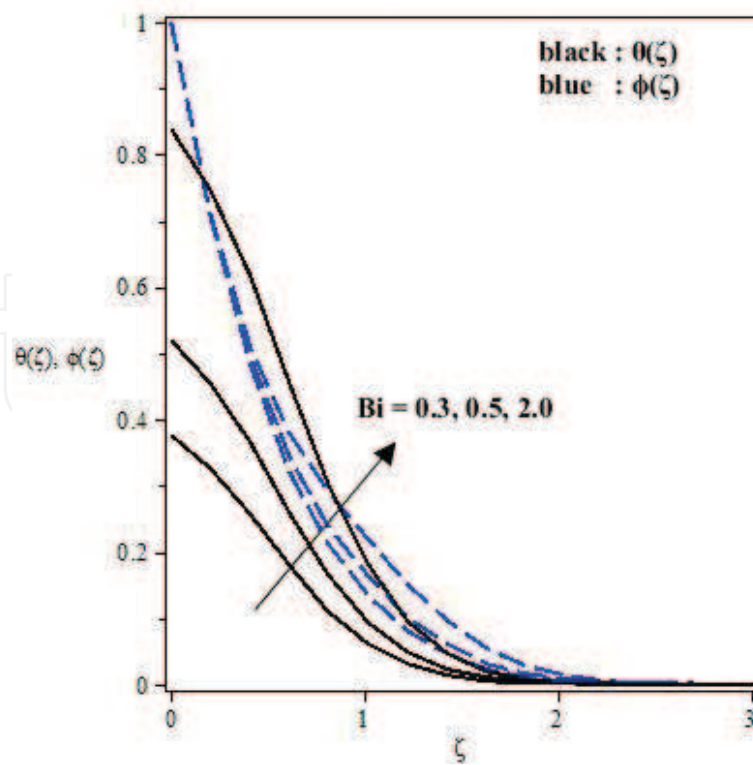


Figure 14. Influence of Bi on temperature and concentration fields.

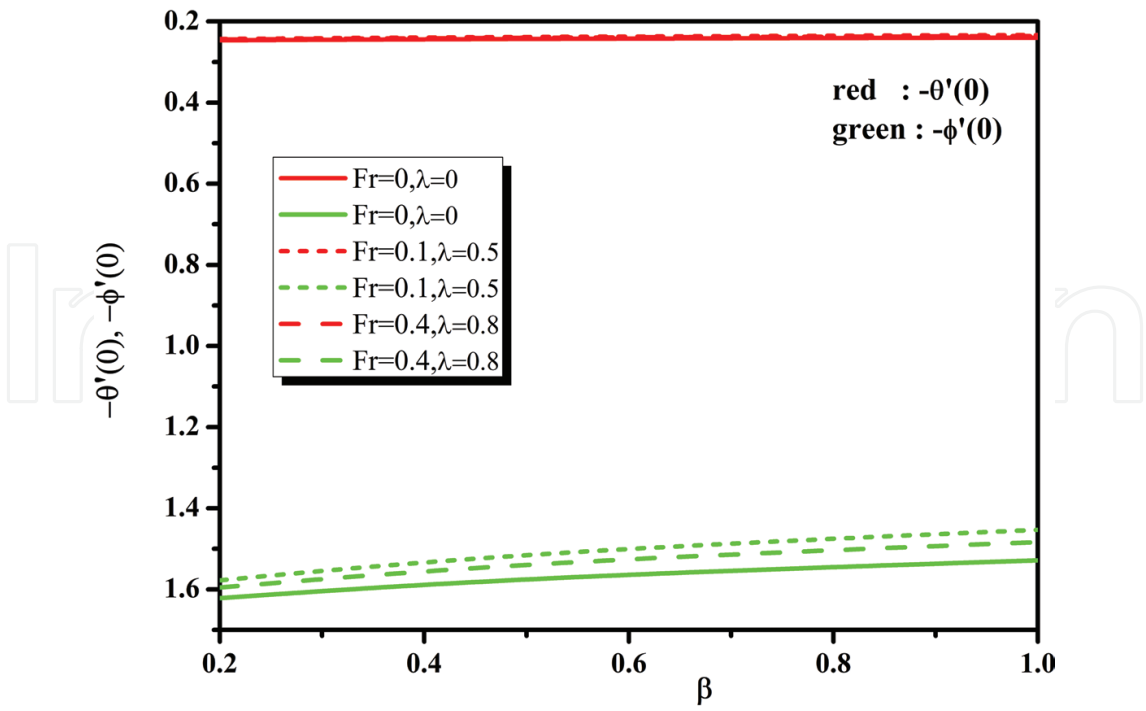


Figure 15. Variation of $-\theta'(0)$ and $-\phi'(0)$ with β for different values of Fr, λ .

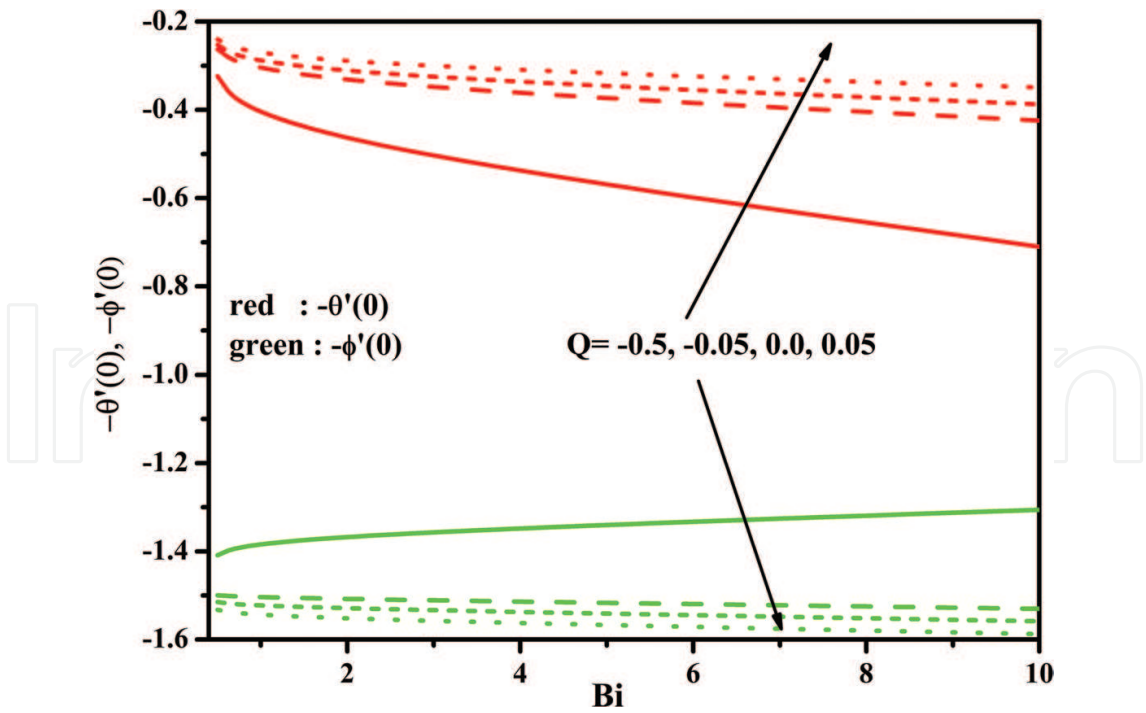


Figure 16. Variation of $-\theta'(0)$ and $-\phi'(0)$ with Bi for different values of Q .

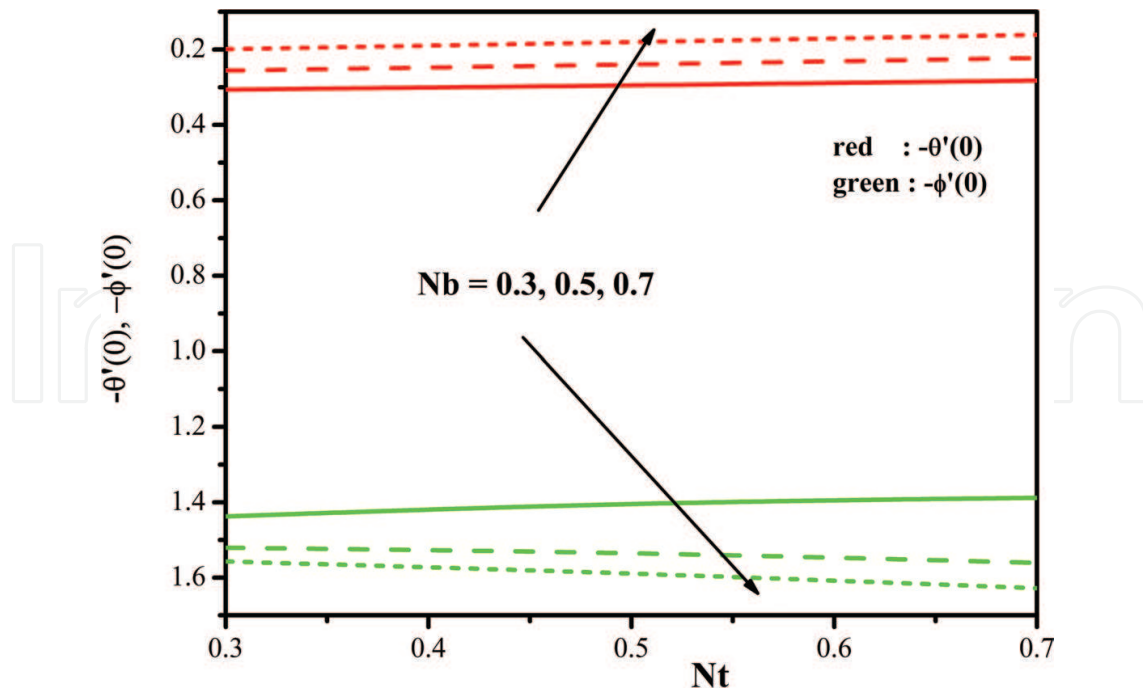


Figure 17. Variation of $-\theta'(0)$ and $-\phi'(0)$ with Nt for different values of Nb .

$\alpha = 1$, sheet will extend along the two bearings with a similar proportion (axisymmetric case), and third and last case identify with extending proportion parameter α other than 0 or 1; at that point, the flow conduct along both directions will be extraordinary.

Attributes of Forchheimer parameter (Fr) on $f'(\zeta)$, $g'(\zeta)$ is plotted in Figure 3. Obviously, $f'(\zeta)$, $g'(\zeta)$ is a diminishing capacity of Fr . Figure 4 features the impact of Fr on $\theta(\zeta)$, $\phi(\zeta)$. Of course $\theta(\zeta)$, $\phi(\zeta)$ and related thickness of boundary layer are higher when Fr increments. Figure 5 illustrates the varieties in $f'(\zeta)$, $g'(\zeta)$ for particular estimations of λ . Both $f'(\zeta)$, $g'(\zeta)$ and related layer thickness decay for larger λ . Physically, nearness of permeable media is to upgrade the protection from smooth movement which makes decay in fluid speed and thickness of energy boundary layer. Figure 6 depicts the impact of λ on $\theta(\zeta)$, $\phi(\zeta)$. It is discovered that bigger λ causes an addition in $\theta(\zeta)$, $\phi(\zeta)$.

Figure 7 showed the impacts of non-Newtonian Casson fluid parameter (β) on velocity profiles $f'(\zeta)$, $g'(\zeta)$. It is seen that with the influence of β infers an abatement in the yield worry of the Casson fluid. This successfully encourages flow of the fluid, i.e., quickens the boundary layer flow near the extending surface, as appeared in Figure 7. In addition, it is found that with substantial estimations of β , the fluid is nearer to the Newtonian fluid. Truth be told, expanding estimations of the Casson fluid parameter β upgrade both temperature and nanoparticle division which is shown in Figure 8.

The variety in dimensionless temperature profile $\theta(\zeta)$ with expanding estimations of generalized Prandtl number Pr is appeared through Figure 9. The temperature profile diminishes

with an expansion in the estimations of Prandtl number Pr , as Prandtl number is the proportion of energy diffusivity to thermal diffusivity. So, an expanding estimation of Prandtl number Pr infers a moderate rate of thermal dissemination which thus lessens the thermal boundary layer thickness. It can be directly seen that Prandtl number has more noticeable impact on Newtonian liquid when contrasted with non-Newtonian liquid.

Figure 10 displays the temperature $\theta(\zeta)$ and the nanoparticle division $\phi(\zeta)$ for variable estimations of Brownian movement Nb . The fluid velocity is found to increment with expanding Nb , while in nanoparticle fraction decreases as Nb expansion which consequently improves the nanoparticle's concentration at the sheet. This might be because of the way the Brownian movement parameter diminishes the mass exchange of a nanofluid. The diagram of thermophoresis parameter Nt on the temperature $\theta(\zeta)$ and the nanoparticle part $\phi(\zeta)$ profiles is portrayed in **Figure 11**. From these plots, it is seen that the impact of expanding estimations of Nt is to build the temperature and nanoparticle fraction.

Figure 12 shows the impact of Lewis number Le on temperature $\theta(\zeta)$ and the nanoparticle portion $\phi(\zeta)$ profiles. It is take note of that the temperature of the liquid increments however nanoparticle portion of the fluid diminishes with increment in Le . Physically truth that the bigger estimations of Lewis number makes the mass diffusivity littler, subsequently it diminishes the fixation field. The impacts of heat source/sink parameter Q can be found in **Figure 13**. For $Q > 0$ (heat source), it can be seen that the thermal boundary layer produces the vitality, and this causes the temperature in the thermal boundary layer increments with increment in Q . Though $Q < 0$ (heat sink) prompts diminish in the thermal boundary layer. $Q = 0$ speaks to the nonattendance of heat source/sink.

Impacts of the Biot number (Bi) on temperature are shown in **Figure 14**. Physically, the Biot number is communicated as the convection at the surface of the body to the conduction inside the surface of the body. At the point when thermal angle is connected at first glance, the proportion representing the temperature inside a body fluctuates significantly, while the body heats or cools over a period. Regularly, for uniform temperature field inside the surface, we consider $Bi \ll 1$. In any case, $Bi \gg 1$ portrays that temperature field inside the surface is not uniform. In **Figure 14**, we have examined the impacts of Biot number Bi on the temperature and nanoparticle portion profiles in two ways. The first one is the situation.

when $Bi < 1$. It is seen from **Figure 14** that for the littlest estimations of the Biot number $Bi < 1$, the variety of temperature inside the body is slight and can sensibly be approximated as being uniform. While in the second case, $Bi > 1$ delineates that the temperature inside the body is not performing a uniform conduct (see **Figure 14**).

The impact of physical parameter on nearby Nusselt $-\theta'(0)$ and Sherwood number $-\phi'(0)$ is displayed in **Figure 15**. We can see through **Figure 15** that non-Darcy-Forchheimer connection creates the low heat and mass at the divider when contrasted with the Darcy-Forchheimer connection. Thus, it is seen with an expansion of the two reasons for speeding up in the λ and Fr . From **Figure 16**, the expanding estimations of the heat source/sink parameter (Q) improve the local Nusselt number $-\theta'(0)$ and decrease the local Sherwood number $-\phi'(0)$ with Bi . A similar conduct is likewise found for the variety in Nt and Nb which is portrayed in **Figure 17**.

4. Conclusions

Three-dimensional flow of Casson nanofluid within the sight of Darcy-Forchheimer connection, uniform warmth source/sink, and convective type boundary condition is considered. Numerical plan prompts the arrangements of physical marvel. From this investigation, we analyzed that the expanding Casson parameter compares to bring down velocity and higher temperature fields. The nearness of Fr and λ caused a lessening in velocity and increasing speed on temperature and nanoparticle portion. The bigger Biot number improved the temperature and nanoparticle division. Additionally, for vast estimations of Biot number, there are no noteworthy changes in $-\theta'(0)$ and $-\phi'(0)$, which are available in **Table 3**. In heat exchange issues, heat sink parameter controls the relative thickening of the force and the thermal boundary layers.

Bi	$-\theta'(0)$	$-\phi'(0)$
0.1	0.084997	1.521377
0.5	0.239615	1.532624
2	0.324388	1.568759
5	0.343057	1.582440
10	0.349174	1.587619
50	0.353999	1.591990
100	0.354597	1.592550
500	0.355075	1.593001
1000	0.355134	1.593057
5000	0.355182	1.593102
10,000	0.355188	1.593108
100,000	0.355193	1.593113
1,000,000	0.355194	1.593113
5,000,000	0.355194	1.593114

Table 3. Computational values of local Nusselt number and local Sherwood number for several values of Bi .

Author details

Gosikere Kenchappa Ramesh

Address all correspondence to: gkrmaths@gmail.com

Department of Mathematics, School of Engineering, Presidency University, Bengaluru, Karnataka, India

References

- [1] Crane LJ. Flow past a stretching plate. *Zeitschrift für angewandte Mathematik und Physik*. 1970;**21**(4):645-647. DOI. org/10.1007/BF01587695
- [2] Grubka LG, Bobba KM. Heat transfer characteristics of a continuous stretching surface with variable temperature. *Journal of Heat Transfer*. 1985;**107**(1):248-250. DOI: 10.1115/1.3247387
- [3] Ali ME. Heat transfer characteristics of a continuous stretching surface. *Heat and Mass Transfer*. 1994;**29**(4);227-234. DOI.org/10.1007/BF01539754
- [4] Gupta PS, Gupta AS. Heat and mass transfer on a stretching sheet with suction or blowing. *Canadian Journal of Chemical Engineering*. 1977;**55**:744746. DOI: 10.1002/cjce.5450550619
- [5] Gireesha BJ, Ramesh GK, Subhas Abel M, Bagewadi CS. Boundary layer flow and heat transfer of a dusty fluid flow over a stretching sheet with non-uniform heat source/sink. *International Journal of Multiphase Flow*. 2011;**37**(8):977-982. DOI.org/10.1016/J.ijmultiphaseflow.2011.03.014
- [6] Ramesh GK, Gireesha BJ. Flow over a stretching sheet in a dusty fluid with radiation effect. *ASME Journal of Heat transfer*. 2013;**135**(10):102702(1-6). DOI: 10.1115/1.4024587
- [7] Bataller RC. Radiation effects for the Blasius and Sakiadis flows with a convective surface boundary condition. *Applied Mathematics and Computation*. 2008;**206**:832-840. DOI.ORG/10.1016/J.AMC.2008.10.001
- [8] Gorla RSR, Sidawi I. Free convection on a vertical stretching surface with suction and blowing. *Applied Science Research*. 1994;**52**:247-257. DOI.org/10.1007/BF00853952
- [9] Ochoa MV. Analysis of drilling fluid rheology and tool joint effects to reduce errors in hydraulics calculations [thesis]. Texas A&M University; 2006
- [10] Nadeem S, Rizwan Ul Haq, Lee C. MHD flow of a Casson fluid over an exponentially shrinking sheet. *Scientia Iranica B*. 2012;**19**(6):1550-1553. DOI.ORG/10.1016/J.SCIENT.2012.10.021
- [11] Mukhopadhyay S. Casson fluid flow and heat transfer over a nonlinearly stretching. *Chinese Physics B*. 2013;**22**(7):074701. DOI.ORG/10.1088/1674-1056/22/7/074701
- [12] Hayat T, Shehzad SA, Alsaedi A, Alhothuali MS. Mixed convection stagnation point flow of casson fluid with convective boundary conditions. *Chinese Physical Letter*. 2012;**29**(11);114704. DOI.org/10.1088/0256-307x/29/11/114704
- [13] Ramesh GK, Ganesh Kumar K, Shehzad SA, Gireesha BJ. Enhancement of radiation on hydromagnetic Casson fluid flow towards a stretched cylinder with suspension of liquid-particles. *Canadian Journal of Physics*. 2018;**96**(1);18-24. DOI.ORG/10.1139/CJP-2017-0307

- [14] Maity S, Singh SK, Kumar AV. Unsteady three dimensional flow of Casson liquid film over a porous stretching sheet in the presence of uniform transverse magnetic field and suction/injection. *Journal of Magnetism and Magnetic Material*. 2016;**419**:292-300. DOI.ORG/10.1016/J.JMMM.2016.06.004
- [15] Nadeem S, Haq RU, Akbar NS, Khan ZH. MHD three-dimensional Casson fluid flow past a porous linearly stretching sheet. *Alexandria Engineering Journal*. 2013;**52**:577-582. DOI.ORG/10.1016/J.AEJ.2013.08.005
- [16] Ahmad K, Nazar R. Magnetohydrodynamic three dimensional flow and heat transfer over a stretching surface in a viscoelastic fluid. *Journal of Science and Technology*. 2011; **3**(1):33-46
- [17] Ramesh GK, Gireesha BJ, Shehzad SA, Abbasi FM. Analysis of heat transfer phenomenon in magnetohydrodynamic Casson fluid flow through Cattaneo-Christov heat diffusion theory. *Communications in Theoretical Physics*. 2017;**68**:91-95. DOI.ORG/10.1088/0253-6102/68/1/91
- [18] Mustafa M, Hayat T, Pop I, Aziz A. Unsteady boundary layer flow of a Casson fluid due to an impulsively started moving flat plate. *Heat Transfer-Asian Research*. 2011;**40**(6): 563-576. DOI: 10.1002/htj.20358
- [19] Buongiorno J. Convective transport in nanofluids. *ASME Journal of Heat transfer*. 2006; **128**:240-250. DOI: 10.1115/1.2150834
- [20] Ahn HS, Kim MH. A review on critical heat flux enhancement with nanofluids and surface modification. *Journal of Heat Transfer*. 2012;**134**:024001. DOI: 10.1115/1.4005065
- [21] Makinde OD, Aziz A. Boundary layer flow of a nanofluid past a stretching sheet with a convective boundary condition. *International Journal of Thermal Science*. 2011;**50**: 1326-1332. DOI.ORG/10.1016/J.IJTHERMALSCI.2011.02.019
- [22] Hsiao KL. Nanofluid flow with multimedia physical features for conjugate mixed convection and radiation. *Computers and Fluids*. 2014;**104**:1-8. DOI.ORG/10.1016/J.COMPFLUID.2014.08.001
- [23] Kuznetsov AV, Nield DA. Natural convective boundary layer flow of a nanofluid past a vertical plate: A revised model. *International Journal of Thermal Science*. 2014;**77**: 126-129. DOI.ORG/10.1016/J.IJTHERMALSCI.2013.10.007
- [24] Hayat T, Muhammad T, Alsaedi A, Alhuthali MS. Magnetohydrodynamic three dimensional flow of viscoelastic nanofluid in the presence of nonlinear thermal radiation. *Journal of Magnetism and Magnetic Materials*. 2015;**385**:222-229. DOI.ORG/10.1016/J.JMMM.2015.02.046
- [25] Ramesh GK, Roopa GS, Gireesha BJ, Shehzad SA, Abbasi FM. An electro-magneto-hydrodynamic flow Maxwell nanoliquid past a Riga plate: A numerical study. *Journal of the Brazilian Society of Mechanical Sciences and Engineering*. 2017;**39**(11):4547-4554. DOI.org/10.1007/s40430-017-0900-z

- [26] Ramesh GK, Prasannakumara BC, Gireesha BJ, Shehzad SA, Abbasi FM. Three dimensional flow of Maxwell nanofluid past a bidirectional porous stretching surface with thermal radiation. *Thermal Science and Engineering Progress*. 2017;**1**:6-14. DOI.ORG/10.1016/J.TSEP.2017.02.006
- [27] Ramesh GK, Gireesha BJ. Influence of heat source/sink on a Maxwell fluid over a stretching surface with convective boundary condition in the presence of nanoparticles. *Ain Shams Engineering Journal*. 2014;**5**:991-998. DOI.ORG/10.1016/J.ASEJ.2014.04.003
- [28] Forchheimer P. Wasserbewegung durch boden. *Zeitschrift des Vereins deutscher Ingenieure*. 1901;**45**:1782-1788
- [29] Muskat M. *The Flow of Homogeneous Fluids Through Porous Media*. New York: McGraw Hill; 1937
- [30] Pal D, Mondal H. Hydromagnetic convective diffusion of species in Darcy-Forchheimer porous medium with non-uniform heat source/sink and variable viscosity. *International Communication in Heat and Mass Transfer*. 2012;**39**:913-917. DOI.ORG/10.1016/J.ICHEATMASSTRANSFER.2012.05.012
- [31] Hayat T, Muhammad T, Al-Mezal S, Liao SJ. Darcy-Forchheimer flow with variable thermal conductivity and Cattaneo-Christov heat flux. *International Journal of Numerical Methods for Heat and Fluid Flow*. 2016;**26**:2355-2369. DOI.ORG/10.1108/HFF-08-2015-0333
- [32] Vishnu Ganesh N, Abdul Hakeem AK, Ganga B. Darcy-Forchheimer flow of hydro-magnetic nanofluid over a stretching/shrinking sheet in a thermally stratified porous medium with second order slip, viscous and Ohmic dissipations effects. *Ain Shams Engineering Journal*. 2016. DOI.ORG/10.1016/J.ASEJ.2016.04.019 (In press)
- [33] AdilSadiq M, Hayat T. Darcy-Forchheimer flow of magneto Maxwell liquid bounded by convectively heated sheet. *Results in Physics*. 2016;**6**:884-890. DOI.ORG/10.1016/J.RINP.2016.10.019
- [34] Ishak A, Nazar R, Pop I. Magnetohydrodynamic (MHD) flow and heat transfer due to a stretching cylinder. *Energy Conversion and Management*. 2008;**49**:3265-3269. DOI.ORG/10.1016/J.ENCONMAN.2007.11.013
- [35] Pal D, Mondal H. Influence of chemical reaction and thermal radiation on mixed convection heat and mass transfer over a stretching sheet in Darcian porous medium with Soret and Dufour effects. *Energy Conversion and Management*. 2012;**62**:102-108. DOI.ORG/10.1016/J.ENCONMAN.2012.03.017